Incompressible liquid based Force sensible silicone retractor attachable to surgical suction instruments

Toshio Koyama, Takeshi Yoneyama, Mitsutoshi Nakada, and Tetsuyou Watanabe, *Member, IEEE*

***Abstract*— This paper presents a silicone retractor, which is a continuation and extension of a previously developed system that had the same three functions as the old version: 1) retracting, 2) suction, and 3) force sensing. These features make the retractor a safe choice for use in neurosurgery. Suction is achieved by attaching the retractor to a suction pipe. The retractor has a deformation area filled with an incompressible liquid that is displaced in proportion to the extent of deformation; fiberscopes or human eyes detecting the displacement get a visual representation of the force. The new design improves on the old one in three ways—miniaturization, made possible by the incompressible-liquid-based mechanism, and measurement of force distribution by distribution of the areas deformed by force. The system was validated by conducting experiments.**

I. Introduction

Recently, several instruments are used in the medical field, e.g., electric scalpel, bipolar, endoscope, and suction device. The number of different tools available leads to an increase in the number of times an instrument is changed. Instrument changes can disturb a surgeon's concentration and increase the operation time for surgery, which presents a burden to the patients. Hence, a reduction in the number of times an instrument is changed is required.

A possible approach could involve embedding multiple functions in an instrument. Based on this concept, we previously developed a silicone retractor that could be used by attaching it to the tip of the suction pipe [1] as shown in Fig. 1. To prevent surgeons from applying an overload on a tissue, the retractor had a force sensing function in addition to retraction and suction. This function is important to avoid damaging a normal (brain) tissue. The deformation part was embedded in the silicone retractor. This part deformed when load was applied to the retractor. Cameras or fiberscopes visually captured the deformation. The system was based on a force visualization mechanism [2]–[4]. However, the system drawbacks included the large thickness of the retractor, which decreased the retracting function and limited the number of applicable cases.

This paper presents an extended version of the silicone retractor that solved this issue. The key features of the new silicone retractor include the following.

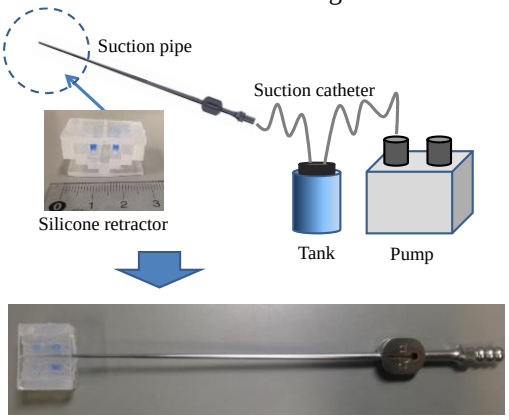

Figure 1. Silicone retractor with the multifunctions of retraction, suction, and force sensing as developed in a previous study.

Force visualization mechanism utilizing incompressible liquid: Incompressible liquid was installed into the retractor. The tube was connected to the retractor to observe liquid level, which is displaced accordance to the load. The load could be visually captured by the liquid displacement. The liquid-based system facilitated miniaturization of the force sensor parts. This was a key element in reducing the thickness.

Distributed force measurement: The miniaturization of the force sensor parts enabled the embedding of five force sensor parts in different areas of the silicone retractor. Consequently, the distributed forces were measurable.

High usability: In a manner similar to extant literature [1], the silicone retractor could be easily set up by installing a suction pipe into the retractor's hole. The retractor was composed entirely of silicone and connected to PTFE tubes. Thus, the system benefits included the absence of electrical components, disposability, easy sterilization/disinfection, MRI compatibility, and low cost.

Multiple functions: In keeping with the retractor developed in a previous study [1], the current retractor also simultaneously provided the functions of retraction, suction, and force sensing via attachment to the suction pipe.

The rest of this paper is organized as follows. The subsequent related works are presented followed by a description of the proposed system. The experimental calibration and validation are detailed. Finally, the results are

*Research supported by JST Astep AS262Z01299K and JSPS KAKENHI Grant Number 16H04298.

T. Koyama is with the Department of mechanical Engineering, College of science and engineering, Kanazawa University, Ishikawa, Japan (corresponding author to provide e-mail: toshio83@stu.kanazawa-u.ac.jp).

T. Yoneyama, and T. Watanabe are with School of Mechanical Engineering, College of Science and Engineering, Kanazawa University, Ishikawa, Japan (e-mail: yoneyama@t.kanazawa-u.ac.jp; te-watanabe@ieee.org)

M. Nakada is with Faculty of Medicine, Institute of Medical, Pharmaceutical and Health Sciences, Kanazawa University, Ishikawa, Japan.

summarized.

A. *Related works*

This paper involves novel medical instruments with the multifunctions of retraction, suction, and force sensing. This paper focused on the key mechanism involved, namely, the force sensing system. Several force sensing systems related to medical operations were developed by extant literature. A detailed analysis can be obtained from several review papers [5]–[11]. The commonly used force sensing systems are based on strain gauges [12]–[14]. Further, tactile/force sensing systems based on magnet and magnetic sensors were developed [15], [16]. Electrical components are not preferable in medical operations due to the requirement of sterilization or disinfection. Moreover, magnetic components are not preferable in medical operations because of the MR incompatibility. Additionally, large amplifiers and other related components are required for the measurement. This increases the size of the system as a whole and subsequently increases the cost. Several approaches were proposed to resolve these issues.

Takaki et al. utilized moiré fringe patterns to visually display force information on forceps [17]. A pneumatic force could be transferred via an air tube. Hence, a forceps with a force sensing system and a tip area without electrical components was developed [18], [19]. With respect to stiffness sensors, Kawahara et al. utilized air pressure and a camera/endoscope for estimating organ stiffness [20]. Acoustic information could also be transferred without any electrical components. Fukuda et al. utilized acoustic reflection for estimating tissue softness [21]. Additionally, optical information could be transferred from the tip to the roots of the forceps without any electrical components. Peirs et al. utilized optical fibers to transfer the visualized deformation of a flexible structure [22]. Tada et al. detected the peak illumination changes of a light source embedded to a deformable structure [23]. Ohka et al. tracked the position and orientation of columnar and conical feelers made of silicone through a camera [24]. Kamiyama et al. estimated the motion of two layered markers with cameras to obtain the magnitude, distribution, and direction of load [25]. We utilized high elastic fabric for visualizing a small force magnitude [2], [3]. We also proposed a stiffness sensing system based on the force visualization mechanism [4].

II. FORCE SENSING SYSTEM

A. *Target situation*

This study proposes a medical instrument with the aim of supporting suction and retraction in neurosurgery. Suction devices are used to suck blood, saline, and soft tumor. A retractor is used to retract tissues to extend the visible field for surgeons. Operations with both devices are very popular and frequent in neurosurgery; thus, frequent instrument changes are commonly required. The effort of the surgeons is reduced by combining the two functions in an instrument. Moreover, embedding force sensing and display are useful in realizing safer and easier operations. Fig. 2 shows an example in which two functions, suction and retraction, are combined. The silicone retractor is attached to the suction pipe, and surgeons can handle the two functions without changing the instrument by operating the suction pipe.

Fig. 3 shows the target situation where a silicone retractor attached on the tip of a suction pipe pulls fluids (for instance, blood in Fig. 3), thereby retracting periphery tissue. As the silicone retractor has width, it can retract the tissue. Furthermore, an incompressible liquid was embedded into the silicone retractor for force sensing. The sensor parts were connected to tubes. If a (retracting) force was applied to the retractor, the sensor parts deformed and the liquid level changed. The change in liquid level inside the tubes could be visually captured. However, the liquid level can be different depending on the instrument's angle. In addition, surgeons may not be able to detect small changes in the liquid level. Therefore, the quantitative force value could be obtained if a camera or fiberscope that is fixed on the suction pipe was used. Surgeons could also approximately understand the magnitude of the retracting force by observation and avoid the fracture in normal tissues due to an overload.

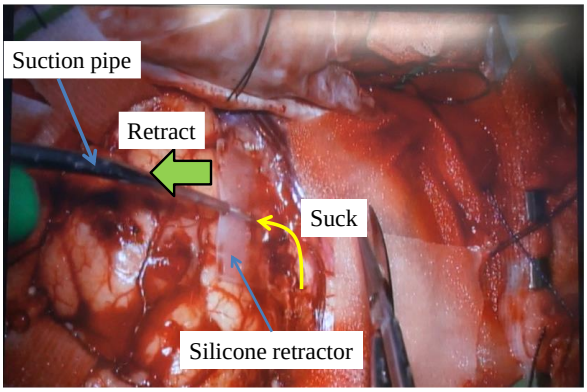

Figure 2. How to use silicone retractor attached to the suction pipe

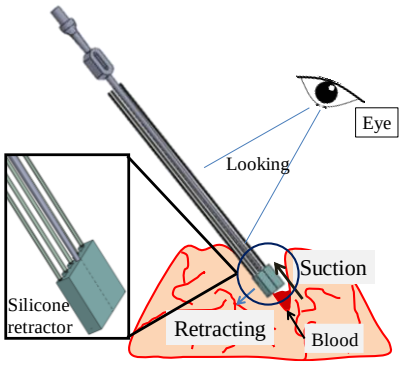

Figure 3. Target situation

B. *Design requirements*

1. Suction, retraction, and retracting force measurement are available simultaneously.
2. There is no electrical component in the silicone retractor.
3. The silicone retractor can be attached to the suction

pipe.

4. The force can be visually captured at the area away from the tissue (retraction and suction areas).
5. The dimensions should include a width of less than 25 mm, length of less than 15 mm, and thickness of less than 4 mm.
6. The force range should be 0.00 N–1.00 N, and the resolution should be 0.05 N.
7. Distributed forces could be measured.

The above points are the design requirements for the silicone retractor that included the force sensing function. We realized the three functions by attaching the force sensing silicone retractor to the suction pipes. The absence of electrical components in the silicone retractor led to several advantages including easy setup, disposability, easy sterilization/disinfection, MRI compatibility, and low cost.

The force visualization mechanism was used so that surgeons could directly visualize the magnitude of the retracting force and avoid an overload on the tissues. In the previously developed system [1], visualized force information was displayed on the silicon retractor. However, there were some cases where the silicon retractor could not be seen due to spreading blood or the occlusion of the periphery tissue that covered the retractor. To resolve this issue, the captured area for the visualized force was set away from the tissues.

This paper contributed in reducing the dimensions. The previously developed retractor [1] had dimensions of a width of 28 mm, length of 20 mm, and thickness of 15 mm. In this paper, the requirement for thickness was dramatically reduced to 4 mm. Thus, the proposed system was available in a deep and narrow space where the previous system could not be applied. The required range and resolution were the same as the previous system [1] and were based on the studies of Budday et al. [26]. The main objective included avoiding overload, and the resolution of 0.05 [N] was considered to be sufficiently accurate. In the previous system [1], only the total force at the center area of the retractor (around the suction pipe) could be measured. There could be the cases where the target tissue was nonuniform, and hence force distribution was not uniform. To avoid fractures, measurement of distributed forces is preferable.

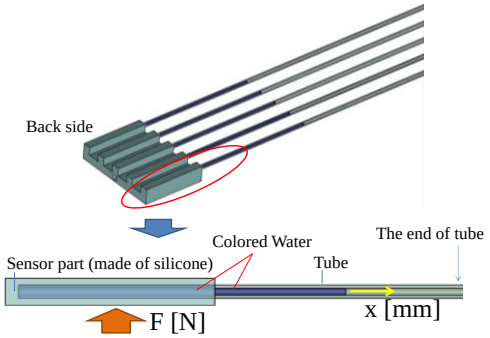

Figure 4. Principle of force sensing.

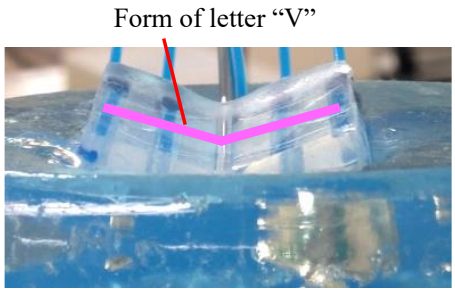

Figure 5. Shape of deformation for the developed force sensible silicone retractor.

C. *Principle of force sensing*

Fig. 4 shows a schematic of the principle of force sensing. A silicone bag filled with incompressible liquid (water) was used to construct the sensor part. The internal portion of the sensor was connected to the tube. The tube end was open so that water could freely move inside the tube. If force was applied at the sensor part, it deformed and water moved toward the tube end due to the incompressibility of water. Moreover, thanks to surface tension, the water level does not change because of the motion of tube. Therefore, the moving distance of water could be used to estimate the magnitude of the applied force. The diameter of the tubes was so small that the moving distance of water could be captured. Note that this method was valid when the pressure of the magnitude (the stiffness of the sensor part) was equal to or lower than the contact pressure (the stiffness of the target object/tissue), as indicated by previous experimental results [27]. Therefore, the system could have a dead zone where the water does not move even if load was applied to the system. The dead zone appeared when the load was small, specifically 0–0.2 [N]. Therefore, it was not a problem for avoiding the overload. Furthermore, the system range and resolution depended on the elasticity of the sensor part’s material.

Let F [N] be the magnitude of the retracting force, and x [mm] be the moving distance of the edge of the colored water from the initial position. We calibrated the relationship between F [N] and x [mm] in advance. Then, load (F [N]) could be estimated by the displacement of water (x [mm]). To simplify the detection of the displacement (x [mm]), colored water was used. By tracking the edge of the colored water, the displacement of water (x [mm]) could be determined. The volume of water did not influence the relationship between F [N] and x [mm] on account of the incompressibility of the water.

To measure the distributed forces, the five sensor parts were installed as shown in Fig. 4. The retractor deformed in the form of letter “V,” as can be seen in Fig. 5, when the tissues were retracted with the silicone retractor. This is because the tissues and the silicone retractor are soft; however the suction pipe is hard. Therefore, the force was applied only to a portion of the suction pipe. The five sensor parts were arranged such that the distribution of deformation could be captured.

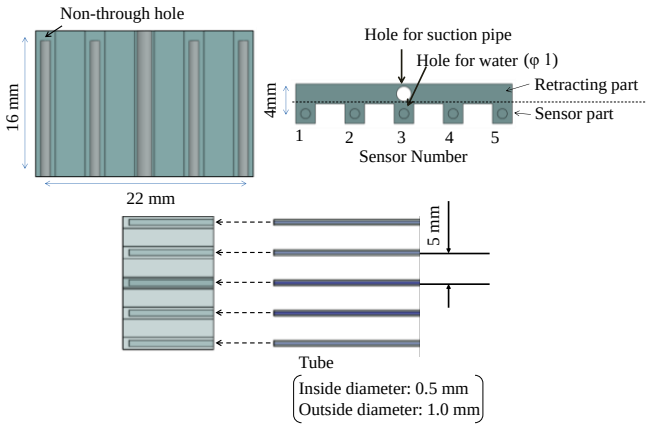

Figure 6. Top and side views for the structure of the force sensing silicone retractor.

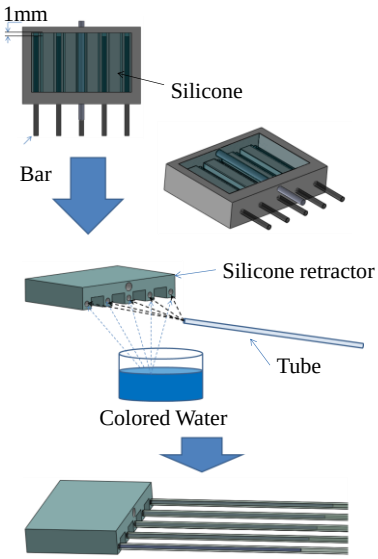

Figure 7. Overiew of the manufacturing and assembly processes for the proposed force sensing silicone retractor.

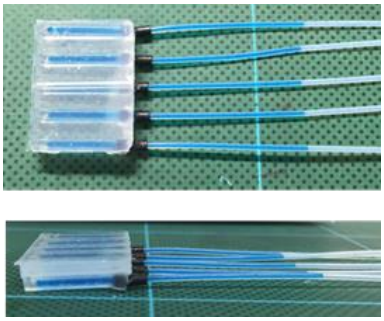

Figure 8. Manufactured force sensing silicone retractor.

D. *Structure of force sensible silicone retractor*

Fig. 6 shows a schematic of the structure of the silicone retractor developed in this paper. As shown in Fig. 6, the retracting part, five sensor parts, colored water, and tube were used to construct the developed silicone retractor. The retracting and sensor parts were made of silicone (Liquid silicone: KE-1308, Hardener: CAT1300, Liquid silicone [g]: Hardener [g] = 1:0.06) produced by Shin-Etsu Co., Ltd. The water was colored by an edible blue colorant (food coloring) produced by Kyoritsu Foods Co. Inc. The used tube was a PTFE tube (TUF-100 series) produced by Chukoh Chemical Industries Ltd. These parts did not include any electrical components and were low cost, disposable, and easy to sterilize/disinfect. The five sensor parts are denoted by No.1, No.2, …., No. 5 in increasing order from left to right in Fig. 6. The dimensions of the developed silicone retractor had a width of 22 mm, length of 16 mm, and thickness of 4 mm.

Fig. 7 shows the overview of the manufacturing and assembly processes of the proposed force sensing silicone retractor. Fig. 8 shows the manufactured force sensing silicone retractor. The retractor and sensor parts were made with a monolithic molding. Initially, liquid silicone was poured into the mold to manufacture the retractor and sensor parts. The bars were inserted into the mold before the liquid silicone solidified. After the silicone solidified, the bars were removed, and the holes for a suction pipe and the sensor parts were obtained. The colored water was poured into the holes of the sensor parts and tubes. Finally, bonding joined the silicone part and the tube. This was a prototype, and a bond (CA-522) produced by CEMEDINE Co., Ltd. was used to glue the tube into the sensors. A biocompatible bond could also be used.

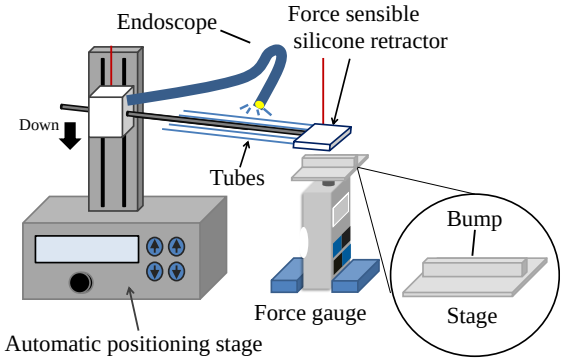

Figure 9. Schematic view of the experimental setup

III. EXPERIMENTAL CALIBRATION

We conducted experiments to derive the relationship between the applied loads on the sensor parts (F [N]) and the moving distance of the edge of the colored water (x [mm]). Fig. 9 shows a schematic of the experimental setup. Fig. 10 shows a photograph of the setup. The developed silicone retractor was attached to a suction pipe. The suction pipe was attached to the automatic positioning stage (IMADA MX2-500N). The force gauge (IMADA MX2-500N) was fixed to measure force in the vertical direction. The handmade stage was placed on the force gauge. The stage had a bump to calibrate the performance of each sensor part, as shown in Fig. 9. The width of bump was the same as that of the sensor part for calibration. The endoscope (Vktech) was attached to the automatic positioning stage so that the photograph of the colored water in the tubes could be captured at the same position (the relative pose and position of the tubes from the endoscope could be the same). Table 1

presents the related specifications of the experimental instruments.

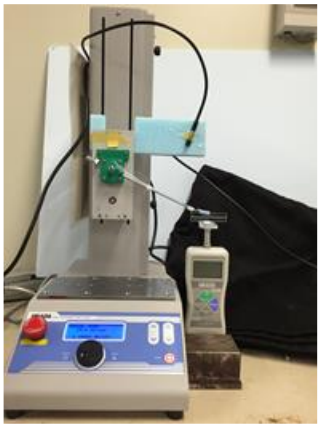

Figure 10. Photo of the experimental set up.

TABLE I. SPECIFICATIONS OF THE EXPERIMENTAL INSTRUMENTS

Instruments	Specification
Endoscope	Resolution: 640 × 480
Force gauge	Resolution: 0.01 N
Automatic positioning stage	Resolution: 0.01 mm Speed: 10 mm/min

A. *Procedure*

The contact between the sensor part of the silicone retractor with the bump of the stage was enabled by the automatic positioning stage. The position of the stage was controlled so that the value of the force gauge was 0.00 N. Then, the automatic positioning stage was controlled to increase the load by an increment of 0.05 N until it reached 1.00 N or the contact (between the bump and sensor part) was lost. As shown in Fig. 5, the silicone deformation increased in the form of a letter "V." Then, a large deformation could result in a deviation of the contact area and lose the contact. The contact was lost when the load was 0.55 N for sensor part Nos. 2 and 4, and 0.2 N for sensor part Nos. 1 and 5. At each step, the photograph of the colored water in the tube was taken to estimate the moving distance of the edge of the colored water. The experiment was repeated five times for every sensor part.

B. *Deviation of the moving distance of the colored water*

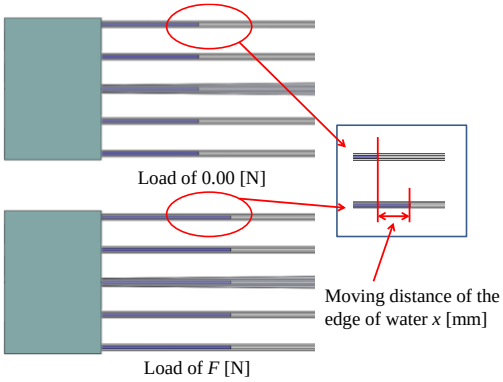

Figure 11. Schematic of the procedure to obtain the moving distance of the colored water in the tube.

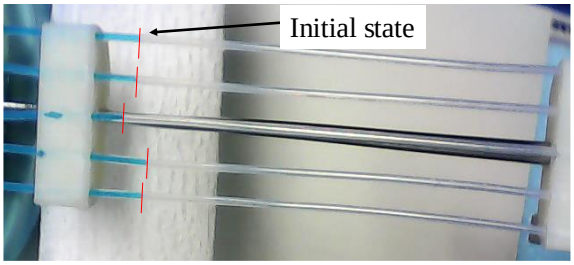

(a) Load of 0.00 [N]

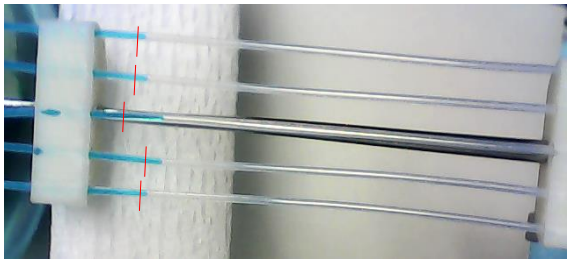

(b) Load of 1.00 [N]

Figure 12. Image of movement of colored water

Fig. 11 illustrates the procedure to derive the moving distance of the colored water. The displacement of the edge corresponding to the moving distance of the colored water was obtained by focusing on the edge of the colored water. As indicated in Fig. 11, the position when the load value was 0.00 N was set as the reference, and the displacement from the reference position was derived. The image analysis was conducted by Adobe Photoshop. Fig. 12 shows images of the load at 0.00 and 1.00 N as representative results.

C. *Calibration based on the experimental results*

Fig. 13 shows the experimental results for the relationship between the applied load (F [N]) and the moving distance of the edge of the colored water (x [mm]). The mean values with the error bar expressing the standard deviation are shown. The following model was used for the regression:

$$F = a_3 x^3 + a_2 x^2 + a_1 x + a_0 \quad (1)$$

where a_0, a_1, a_2, and a_3 are the parameters. The fitting was done by the curve fitting toolbox of Matlab. The parameter values for each sensor part are shown in Table II, while Table III shows the results for the fitting accuracy

From Table III, it could be observed that sufficient fitting accuracy was obtained for the design requirements of the resolution of 0.05 N. As shown in Fig. 13, there were some cases where the increasing rate of the load with respect to the moving distance decreased to become almost flat (constant). This was due to the buckling of the sensor part. To take the effect of the buckling into account, a three-dimensional polynomial function was used as a regression model. The curve for sensor part No.2 was different from that for sensor part No.4. This was due to the manufacturing inaccuracy of hole position, which affected the directions of the applied forces and the corresponding deformation.

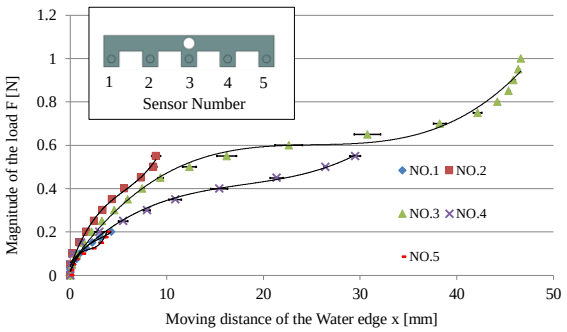

Figure 13. Relationship between the applied load (F [N]) and the moving distance of the edge of the colored water (x [mm]).

TABLE II. PARAMETER VALUES FOR THE REGRESSION MODEL

Number of the sensor part	a_3	a_2	a_1	a_0
No. 1	1.78×10^{-3}	-1.86×10^{-2}	8.76×10^{-2}	2.72×10^{-2}
No. 2	7.32×10^{-4}	-1.33×10^{-2}	1.15×10^{-1}	4.17×10^{-2}
No. 3	3.21×10^{-5}	-2.44×10^{-3}	6.32×10^{-2}	5.17×10^{-2}
No. 4	2.88×10^{-5}	-1.61×10^{-3}	3.80×10^{-2}	9.08×10^{-2}
No. 5	7.74×10^{-3}	-4.51×10^{-2}	1.04×10^{-1}	2.93×10^{-2}

TABLE III. FITTING ACCURACY OF REGRESSION

Number of the sensor part	Coefficient of determination (R^2)	RMSE (Root Mean Squared Error)
No. 1	0.99	0.005
No. 2	0.99	0.025
No. 3	0.99	0.027
No. 4	0.99	0.018
No. 5	0.99	0.006

IV. EXPERIMENTAL EVALUATION

Fig. 14 shows the photograph of the experiment of retracting gelatin. To confirm the validity of the developed force sensing system, we conducted experiments to check whether the applied load could be estimated when retracting gelatin. The experimental setup was the same as the one shown in Fig. 9, except for the stage. The flat stage was used instead of the stage with bump. The gelatin (Maruha Nichiro Corporation, blending ratio: gelatin powder 2 [g] and water 25 [ml]) was located on the stage. Initially, the silicone retractor was in contact with the gelatin with a load of 0.00 N. The load was increased in increments of 0.05 N by controlling the automatic positioning stage. At each step, a photograph was taken to derive the moving distance of the water for each sensor part. The experiment was conducted five times.

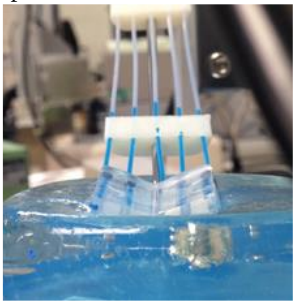

Figure 14. Photo of the experiment of retracting gelatin.

A. Results

Let F_i be the load F for the sensor part No. i and F_i at x is denoted by $F_\mathrm{i}(x)$. The distributed forces ($F_\mathrm{i}(x)$) were calculated by using (1). The total force ($F_\mathrm{t}(x)$) was calculated by the following expression:

$$F_\mathrm{t}(x) = F_1(x) + F_2(x) + F_3(x) + F_4(x) + F_5(x) \qquad (2)$$

We compared the derived total force ($F_\mathrm{t}(x)$) with the actual value of the load. The results were shown in Fig. 15. Fig .16 shows the corresponding distributed forces.

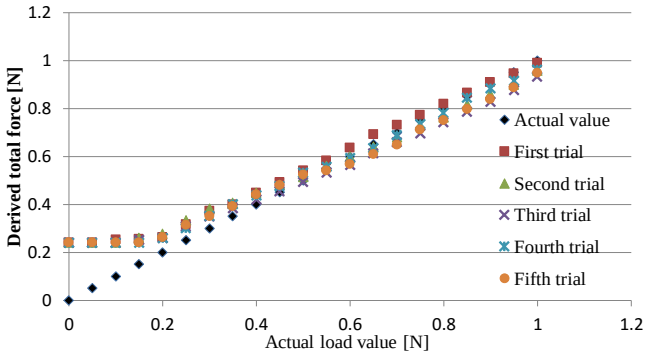

Figure 15. Comparison of the derived total force from the proposed sensing system with the actual value of the load.

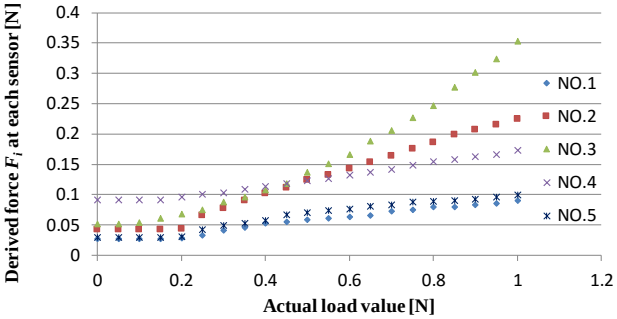

Figure 16. Comparison of each force derived from the proposed sensing system with the actual load value.

B. Discussion

As indicated in Fig. 15, there was a small difference between the derived total force and actual load. A resolution of 0.05 N was obtained, suggesting the validity of the developed force sensing system. The reason for the difference could be the low resolutions of the endoscopes. Note that the force sensing system worked between 0.2 and 1.0 N. As observed in Fig. 13, each sensor could not work in the range 0.0–0.05 N. As illustrated in Fig. 15, the total forces (under 0.2 N) were distributed, and the load for each sensor part became small (under 0.05 N). This could be the reason for the dead zone of 0–0.2 N.

Fig. 16 shows that the distributed forces could be observed. The difference between sensor part Nos. 2 and 4 was due to the manufacturing inaccuracy of the hole position (as mentioned above).

V. CONCLUSION

This paper presented a novel instrument for neurosurgery.

The proposed instrument had three functions: retraction, suction, and force sensing. Suction instruments and retractors are frequently used in neurosurgery. To reduce the number of times an instrument is changed and enhance operation safety, we developed a silicon retractor with force sensing [1]. This worked by attaching the instrument to the tip of a suction pipe. The system had the three key functions, but its large thickness presented a serious problem by limiting its usability. To overcome this drawback, this paper presented a new force sensible silicon retractor, which also worked by attaching it to the suction pipe. The usage of an incompressible liquid was the key solution for reducing the thickness. The sensor part was constructed by a silicone bag with the liquid, namely, colored water. Given the incompressibility, the deformation of the silicon bag resulted in the movement of water. The applied force was estimated by visually detecting the displacement of the colored water. The obtained sensor resolution was less than 0.05 N and the range was 0.05–1.0 N. Other features of the sensor system included its low cost and disposability. Five additional sensor systems were installed for measuring the distributed forces. The experimental results showed the validity of the system. When the total load was derived, the range 0–0.2 N was a dead zone. The dead zone at a low range is not a serious issue in avoiding the overload and ensuring the safety of operations. However, it is preferable for force sensing to be available at a low range. Future work could include the improvement of sensing at a low range.

REFERENCES

[1] T. Koyama, T. Iwai, T. Yoneyama, H. Kagawa, Y. Hayashi, M. Nakada, and T. Watanabe, "Silicone retractor with embedded force-sensing function for attachment to surgical suction pipes," in *2015 IEEE International Conference on Advanced Intelligent Mechatronics (AIM)*, 2015, vol. 2015-Augus, pp. 145–150.

[2] T. Iwai, Y. Fujihira, L. Wakako, H. Kagawa, T. Yoneyama, and T. Watanabe, "Three-axis force visualizing system for fiberscopes utilizing highly elastic fabric," in *2014 IEEE/ASME International Conference on Advanced Intelligent Mechatronics*, 2014, pp. 1110–1115.

[3] T. Watanabe, T. Iwai, Y. Fujihira, L. Wakako, H. Kagawa, and T. Yoneyama, "Force Sensor Attachable to Thin Fiberscopes/Endoscopes Utilizing High Elasticity Fabric," *Sensors*, vol. 14, no. 3, pp. 5207–5220, Mar. 2014.

[4] T. Iwai, T. Koyama, H. Kagawa, T. Yoneyama, and T. Watanabe, "Visualization method based stiffness sensing system for endoscopes," in *2015 37th Annual International Conference of the IEEE Engineering in Medicine and Biology Society (EMBC)*, 2015, pp. 6449–6452.

[5] R. S. Dahiya, G. Metta, M. Valle, and G. Sandini, "Tactile Sensing-From Humans to Humanoids," *IEEE Trans. Robot.*, vol. 26, no. 1, pp. 1–20, Feb. 2010.

[6] M. I. Tiwana, S. J. Redmond, and N. H. Lovell, "A review of tactile sensing technologies with applications in biomedical engineering," *Sensors Actuators A Phys.*, vol. 179, pp. 17–31, 2012.

[7] P. Puangmali, K. Althoefer, L. D. Seneviratne, D. Murphy, and P. Dasgupta, "State-of-the-art in force and tactile sensing for minimally invasive surgery," *Sensors Journal, IEEE*, vol. 8, no. 4, pp. 371–381, 2008.

[8] E. P. Westebring – van der Putten, R. H. M. Goossens, J. J. Jakimowicz, J. Dankelman, E. P. der Putten, R. H. M. Goossens, J. J. Jakimowicz, J. Dankelman, E. P. Westebring – van der Putten, R. H. M. Goossens, J. J. Jakimowicz, and J. Dankelman, "Haptics in minimally invasive surgery-a review," *Minim. Invasive Ther. Allied Technol.*, vol. 17, no. 1, pp. 3–16, Jan. 2008.

[9] A. M. Okamura, "Haptic Feedback in Robot-Assisted Minimally Invasive Surgery," *Curr Opin Urol*, vol. 19, no. 1, pp. 102–107, 2009.

[10] E. Vander Poorten, E. Demeester, P. Lammertse, E. V. B. Vander Poorten, E. Demeester, and P. Lammertse, "Haptic feedback for medical applications, a survey," *Proc. Actuator*, pp. 18–20, 2012.

[11] J. Back, P. Dasgupta, L. Seneviratne, K. Althoefer and H. Liu, "Feasibility Study- Novel Optical Soft Tactile Array Sensing for Minimally Invasive Surgery," in *2015 IEEE/RSJ International Conference on Intelligent Robots and Systems (IROS)*, 2015, pp. 1528 - 1533.

[12] T. Yoneyama, T. Watanabe, H. Kagawa, J. Hamada, Y. Hayashi, and M. Nakada, "Force-detecting gripper and force feedback system for neurosurgery applications," *Int. J. Comput. Assist. Radiol. Surg.*, vol. 8, no. 5, pp. 819–829, Sep. 2013.

[13] Y. Kanada, T. Yoneyama, T. Watanabe, H. Kagawa, N. Sugiyama, K. Tanaka, and T. Hanyu, "Force Feedback Manipulating System for Neurosurgery," in *Procedia CIRP*, 2013, vol. 5, no. 1, pp. 133–136.

[14] Y. Fujihira, T. Hanyu, Y. Kanada, T. Yoneyama, T. Watanabe, and H. Kagawa, "Gripping Force Feedback System for Neurosurgery," *Int. J. Autom. Technol.*, vol. 8, no. 1, pp. 83–94, 2014.

[15] Tomo, T.P.; Somlor, S.; Schmitz, A.; Jamone, L.; Huang, W.; Kristanto, H.; Sugano, S. Design and Characterization of a Three-Axis Hall Effect-Based Soft Skin Sensor. Sensors 2016, 16, 491.

[16] L. Jamone, L. Natale, G. Metta and G. Sandini, Highly sensitive soft tactile sensors for an anthropomorphic robotic hand. IEEE Sensors Journal, Vol. 15, No 8, pp. 4226-4233. 2015

[17] T. Takaki, Y. Omasa, I. Ishii, T. Kawahara, and M. Okajima, "Force visualization mechanism using a Moire' fringe applied to endoscopic surgical instruments," in *2010 IEEE International Conference on Robotics and Automation*, 2010, pp. 3648–3653.

[18] K. Tadano and K. Kawashima, "Development of 4-DOFs forceps with force sensing using pneumatic servo system," in *Robotics and Automation, 2006. ICRA 2006. Proceedings 2006 IEEE International Conference on*, 2006, pp. 2250–2255.

[19] D. Haraguchi, K. Tadano, and K. Kawashima, "A prototype of pneumatically-driven forceps manipulator with force sensing capability using a simple flexible joint," *IEEE Int. Conf. Intell. Robot. Syst.*, pp. 931–936, 2011.

[20] T. Kawahara, S. Tanaka, and M. Kaneko, "Non-contact stiffness imager," *Int. J. Rob. Res.*, vol. 25, no. 5–6, pp. 537–549, May 2006.

[21] T. Fukuda, Y. Tanaka, M. Fujiwara, and A. Sano, "Softness measurement by forceps-type tactile sensor using acoustic reflection," in *2015 IEEE/RSJ International Conference on Intelligent Robots and Systems (IROS)*, 2015, pp. 3791–3796.

[22] J. Peirs, J. Clijnen, D. Reynaerts, H. Van Brussel, P. Herijgers, B. Corteville, and S. Boone, "A micro optical force sensor for force feedback during minimally invasive robotic surgery," *Sensors Actuators A Phys.*, vol. 115, no. 2–3, pp. 447–455, 2004.

[23] M. Tada, S. Sasaki, and T. Ogasawara, "Development of an optical 2-axis force sensor usable in {MRI} environments," *Proceedings of IEEE Sensors*, vol. 2. pp. 984–989, 2002.

[24] M. Ohka, Y. Mitsuya, Y. Matsunaga, and S. Takeuchi, "Sensing characteristics of an optical three-axis tactile sensor under combined loading," *Robotica*, vol. 22, no. 2, pp. 213–221, Mar. 2004.

[25] K. Kamiyama, K. Vlack, T. Mizota, H. Kajimoto, K. Kawakami, and S. Tachi, "Vision-based sensor for real-time measuring of surface traction fields," *IEEE Comput. Graph. Appl.*, vol. 25, no. 1, pp. 68–75, Jan. 2005.

[26] S. Budday, R. Nay, R. de Rooij, P. Steinmann, T. Wyrobek, T. C. Ovaert, and E. Kuhl, "Mechanical properties of gray and white matter brain tissue by indentation," *J. Mech. Behav. Biomed. Mater.*, vol. 46, pp. 318–330, Jun. 2015.

[27] R. Adachi, Y. Fujihira, and T. Watanabe, "Identification of danger state for grasping delicate tofu with fingertips containing viscoelastic fluid," in *2015 IEEE/RSJ International Conference on Intelligent Robots and Systems (IROS)*, 2015, pp. 497–503.